Spin and Forward Physics with the STAR detector: Measurements and Future Plans

David Kapukchyan (for the STAR Collaboration)

E-Mail: dkapu001@ucr.edu

University of California Riverside

Presented at the Workshop of QCD and Forward Physics at the EIC, the LHC, and Cosmic Ray Physics in Guanajuato, Mexico, November 18-21 2019

Abstract

The spin program at the STAR experiment at the Relativistic Heavy Ion Collider (RHIC) has explored many interesting topics and has helped our understanding of nuclear and nucleon structures. In particular, non-vanishing transverse single-spin asymmetry measurements at RHIC and other experiments have shown that there is a rich substructure of the nucleon that needs further exploration in both theory and experiment. The STAR forward upgrade will utilize RHIC's unique capability of colliding polarized proton and heavy ion beams to carry out measurements of Drell-Yan, jets, hadrons in jets, and dijets, among others with improved precision. The new forward system will be in operation for the pp, pA and AA runs starting in Fall 2021 and utilize the latest developments in detector technologies so that they are ready for the Electron-Ion Collider (EIC). The forward upgrade will cover $2.5 < \eta < 4.0$, by installing two new forward tracking systems and a new calorimeter system. The tracking systems will consist of silicon disks and small-strip thin gap chambers. The calorimeter system will consist of a preshower hodoscope, an electromagnetic calorimeter and a hadronic calorimeter. These proceedings will show some of the recent results from STAR's spin program as well as the design and capabilities of the forward upgrade and how it will complement measurements from a future EIC.

1 Introduction

One of the main open questions in nuclear physics today is what is the origin of the proton spin. This question arose from Deep Inelastic Scattering (DIS) experiments that showed that the spin of the quarks is not sufficient to account for the total spin of the proton [1]. The results shown here will highlight some of the work that has been done by the Solenoidal Tracker at RHIC (STAR) to constrain the contribution of the quarks and gluons to the total spin of the proton. Also, I will discuss how the STAR forward upgrade can be used to even further constrain these quantities. Another important question is how we can describe the multi-dimensional landscape of nucleons and nuclei. Transverse momentum dependent PDFs (TMD) are a key aspect of this question. TMDs address how a parton's transverse momentum inside the proton can be related to physics observables. STAR has measured many TMDs and these proceedings will present the results from only one such TMD, transversity via the Collins fragmentation function, and how the forward upgrade aims to improve upon that result.

2 The Relativistic Heavy Ion Collider

The relativistic heavy ion collider (RHIC) at Brookhaven National Laboratory (BNL) is the only polarized pp collider in the world. In addition, as its name suggests, it can also collide various heavy ion species at a range of energies in both collider and fixed target mode. In the last two decades RHIC has collided various mixtures of p, d, ^{3}He, Al, Cu, Zr, Ru, Au, and U at various energies. Proton-proton collisions have taken place at center-of-mass energies ($\sqrt{s}$) of 62, 200, 500, and 510 GeV. Center-of-mass energies per nucleon-nucleon pair ($\sqrt{s_{NN}}$) in pA and AA collisions have reached up to 200 GeV, while fixed target experiments at STAR have reached as low as $\sqrt{s_{NN}} = 3$ GeV.

The RHIC facility consists of the Brookhaven Linear Accelerator (LINAC), a booster, an Alternating Gradient Synchroton (AGS), two main storage rings, and an Electron Beam Ion Source (EBIS). Polarized pp beams start by inserting transversely polarized protons (~95% polarization) into the LINAC followed by the booster that then feeds into the AGS. The AGS is used to further increase the beam energy and then routes the beam into one of the two main storage rings, where the beams may be further accelerated; the two opposite going beams are named blue and yellow. The polarization is maintained both during acceleration and at collision energy using Siberian Snakes located on the AGS and the main storage rings. To reduce systematic uncertainties, the polarization pattern is chosen from a set of well-defined fill patterns that alternate the polarization direction for consecutive bunches or pairs thereof. In addition, spin rotators are located around the interaction region to allow for either transversely or longitudinally polarized pp or pA collisions. Polarimeters within the ring allow continuous measurements of the beam polarization during a RHIC fill, which typically lasts 8 hours. Unpolarized heavy ion beams start in the EBIS that generates the intial ions that go into the LINAC and then follow the same process [2].

The latest transversely polarized pp run was RHIC Run 17 at $\sqrt{s} = 510$ GeV. It has the highest delivered luminosity per week for all pp runs to date. RHIC has been able to provide highly polarized beams, achieving an average polarization of about 50-60%. Also, of interest, is Run 15 that had a mix of longitudinal and transverse spin pp collisions at $\sqrt{s} = 200$ GeV.

3 STAR Detector

The STAR detector is shown in Fig. 1 [3]. STAR has a Time Projection Chamber (TPC) at mid-rapidity $|\eta| < 1.0$ that covers a full 2π in azimuth [4]. It is used for charged particle reconstruction and identification. Just outside the TPC is the Barrel Electromagnetic Calorimeter (BEMC). The BEMC has the same coverage as the TPC and is used for measuring the energies of electrons and photons. The other two detectors at mid-rapidity are the Time Of Flight (TOF), used to improve particle identification from the TPC, and the Muon Telescope Detector (MTD), which is used to detect muons. In addition, there exist global detectors that have multiple functionalities. These are the Beam-Beam Counter (BBC) located at $3.3 < |\eta| < 5.2$ and the Vertex Position Detector (VPD) located at $4.24 < |\eta| < 5.1$. Lastly, the detectors in forward pseudorapidity (blue beam direction) with full 2π azimuth coverage are the Endcap Electromagnetic Calorimeter (EEMC) $1 < \eta < 2$, and the Forward Electromagnetic Calorimeter (FEMC) $2.5 < \eta < 4.0$.

There were some upgrades completed in 2019 that are not visible in Fig. 1. The inner TPC was upgraded which improved $\frac{dE}{dx}$ resolution and increased coverage to $|\eta| < 1.5$. An Endcap

TOF extends coverage to $1.05 < \eta < 1.7$. Lastly, installed in 2018, the Event Plane Detector (EPD) covers $2.1 < |\eta| < 5.1$. It is used to provide event triggers and improve event plane resolution.

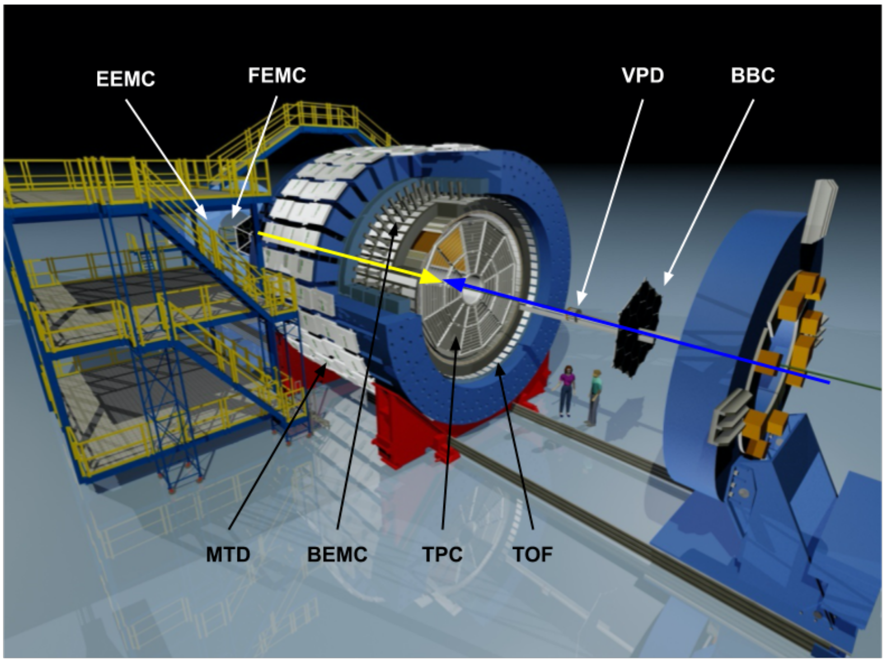

Figure 1: STAR detector and its various detector subsystems. Information on each subsystem can be found in the text.

4 Helicity Structure of Proton

The longitudinal spin of the proton can be decomposed into the various angular momenta of the quarks and gluons that make it up. One such decomposition, the Jaffe-Manohar spin sum rule, decomposes the spin of the proton according to equation (4.1)

$$\frac{1}{2} = \frac{1}{2}\Delta\Sigma + \Delta G + L_z \tag{4.1}$$

where $\Delta\Sigma$ is the quark polarization, ΔG is the gluon polarization and L_z is the orbital angular momentum of the quark-gluon system. The quark polarization can be further broken down into the valence quark and sea quark polarization. The quark polarization has been measured using DIS experiments and accounts for only about 30% of the total proton spin in a limited x range [1]. The EIC will provide better constraints on the valence quark polarization. The sea quark polarization can be probed using the parity violating $W^{\pm}$ production at RHIC. The diagram in Fig. 2 shows how W's are produced. This production is maximally parity violating so the quarks must have opposite helicities. An up quark from one

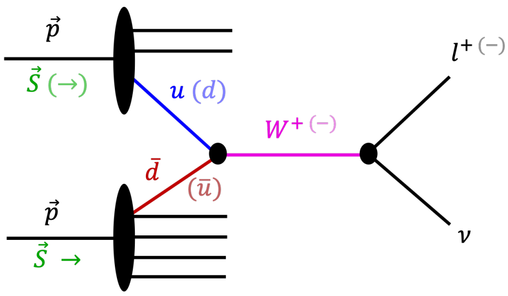

Figure 2: Feynman diagram showing parity violating W production. It requires the $u(d)$ quark must interact with a $\bar{d}(\bar{u})$ quark.

proton must interact with an anti-down quark from the other proton to produce a W or vice versa. This measurement is complementary to Semi-Inclusive DIS (SIDIS) as there is no fragmentation to tag the flavor. STAR measures the single-spin asymmetry A_L (equation (4.2)) of W's via its leptonic decay in longitudinal pp collisions,

$$A_L^{W^+} = \frac{\sigma^+ - \sigma^-}{\sigma^+ + \sigma^-} \sim \frac{\Delta\bar{d}(x_1)u(x_2) - \Delta u(x_1)\bar{d}(x_2)}{\bar{d}(x_1)u(x_2) + u(x_1)\bar{d}(x_2)} \tag{4.2}$$

where the "+" denotes positive helicity and "-" denotes negative helicity. The A_L measurement for $W^\pm$ from STAR in the region $|\eta| < 1.2$ is shown in Fig. 3. The lepton pseudorapidity is used to dial into the sea quark polarization. These data show a positive $\Delta\bar{u}$ in $0.05 < x < 0.25$. Furthermore, the NNPDF reweighting of the new data, shown in Fig. 4 in the blue band, shows a clear sea quark polarization asymmetry $\Delta\bar{u} > \Delta\bar{d}$ [5].

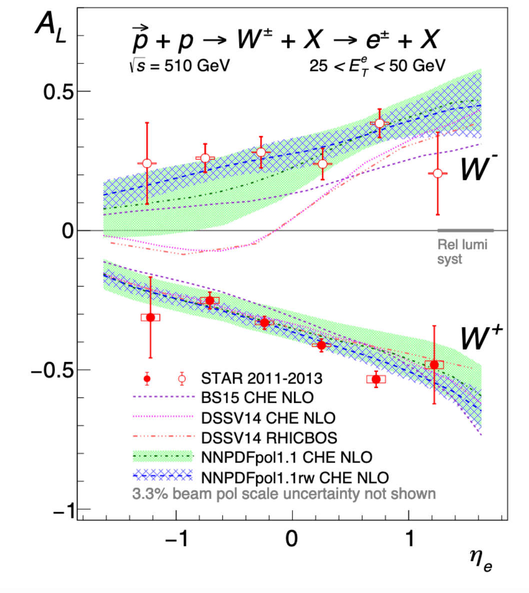

Figure 3: Measured A_L for $W^\pm$ vs. lepton psuedorapidity (η_e) together with theory expectations (curves and bands). Data shown are combined from 2011, 2012 and 2013 [5].

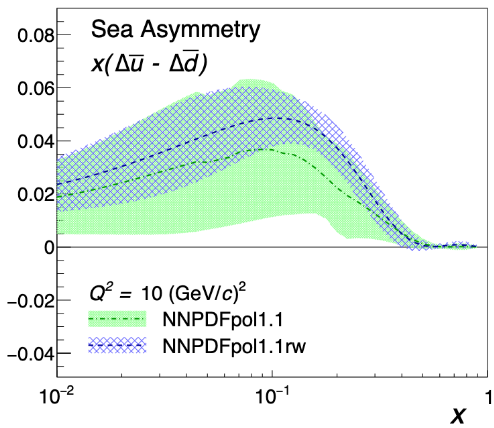

Figure 4: Difference in light sea-quark polarizations as a function of x at $Q^2 = 10$ GeV^2. The green band shows the NNPDFpol1.1 results before the 2013 STAR data shown in Fig. 3. The blue hatched band is a reweighting of the PDF after the 2013 STAR data was included. A clear sea quark polarization asymmetry of $\Delta\bar{u} > \Delta\bar{d}$ is seen [5].

The gluon polarization can be measured using jet, dijet and π^0 production at RHIC. Figure 5 shows the relative fractions of different processes that contribute to inclusive jet production as a function of $x_T = 2p_T/\sqrt{s}$. It shows that at low x_T gluon-gluon subprocesses dominate over the quark-quark subprocesses [6]. The longitudinal double-spin asymmetry (A_{LL}) for inclusive jets, defined in equation (4.3), in this regime is sensitive to the gluon polarization.

$$A_{LL} = \frac{\sigma^{++} - \sigma^{+-}}{\sigma^{++} + \sigma^{+-}} = \frac{1}{P_1 P_2} \frac{N^{++} - RN^{+-}}{N^{++} + RN^{+-}} \tag{4.3}$$

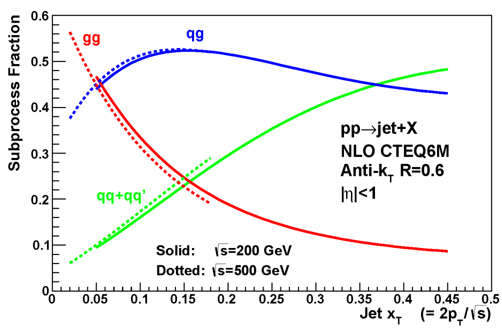

Figure 5: Subprocesses that dominate inclusive jet production as a function of x_T. At low x_T gluon-gluon scattering dominates [6].

In equation (4.3) σ is the inclusive jet cross section, P_1 and P_2 are the polarization of beam 1 and 2 respectively, R is the relative luminosity and N is the number of events with "++" denoting same helicity and "+-" denoting opposite helicity. Measurements of A_{LL} of inclusive jets at STAR mid-rapidity ($|\eta| < 1.0$) are shown in Fig. 6 for both $\sqrt{s} = 200$ GeV and 510 GeV energies. At both energies there is a clear asymmetry at low x_T. These results will provide important new constraints on the magnitude of the gluon polarization [6].

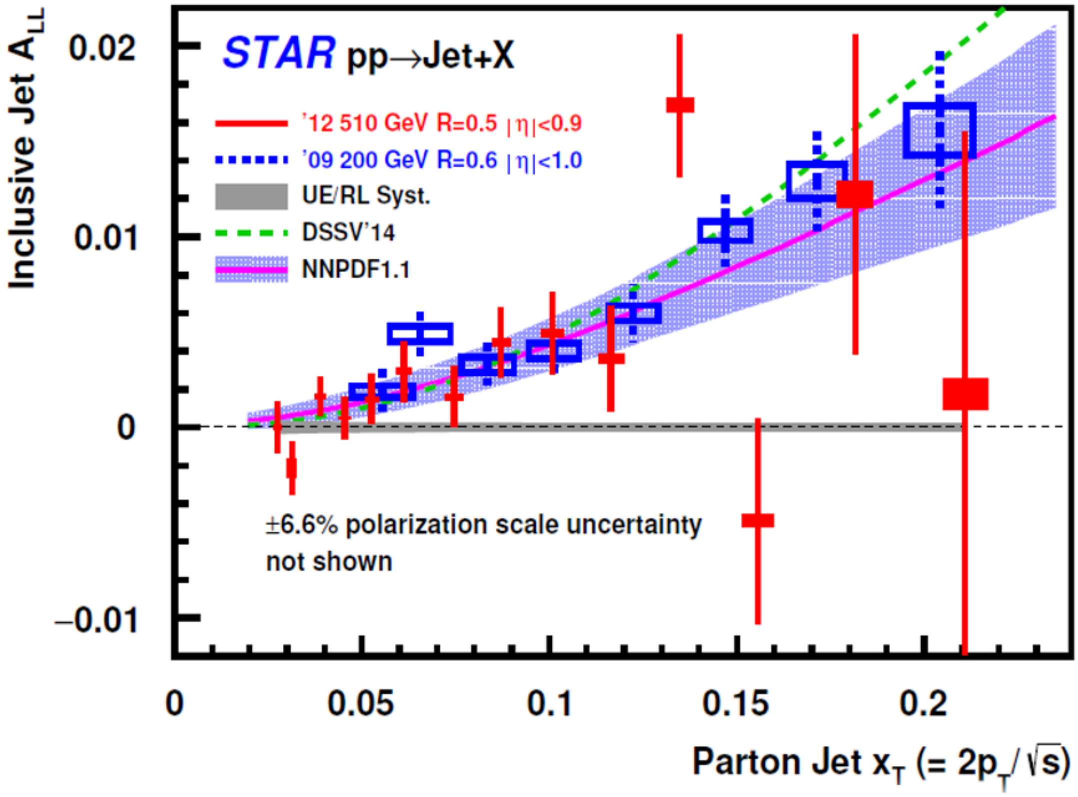

Figure 6: A_{LL} of inclusive jets as a function of x_T, where $x \approx x_T e^{\pm\eta}$. Data are for both 200 GeV and 510 GeV pp collisions. A clear asymmetry exists in the low x_T region [6].

Inclusive di-jet A_{LL} was also measured at STAR at various pseudorapidity bins or topologies. Figure 7 shows the measured A_{LL} in each topology where the designation central corresponds to the pseudorapidity bin $|\eta| < 0.3$ and forward/backward corresponds to $0.3 < |\eta| < 0.9$. It also shows the various x regions probed by the different bins, where

$$x_1 = \frac{1}{\sqrt{s}}(p_{T,3}e^{\eta_3} + p_{T,4}e^{\eta_4}) \tag{4.4a}$$

$$x_2 = \frac{1}{\sqrt{s}}(p_{T,3}e^{-\eta_3} + p_{T,4}e^{-\eta_4}) \tag{4.4b}$$

The x values as shown in the left panel of Fig. 7 become more equal as you go from forward-forward to central-central and forward-backward. These A_{LL} measurements, when combined with global analyses, will help to constrain the shape of $\Delta g(x)$ [6].

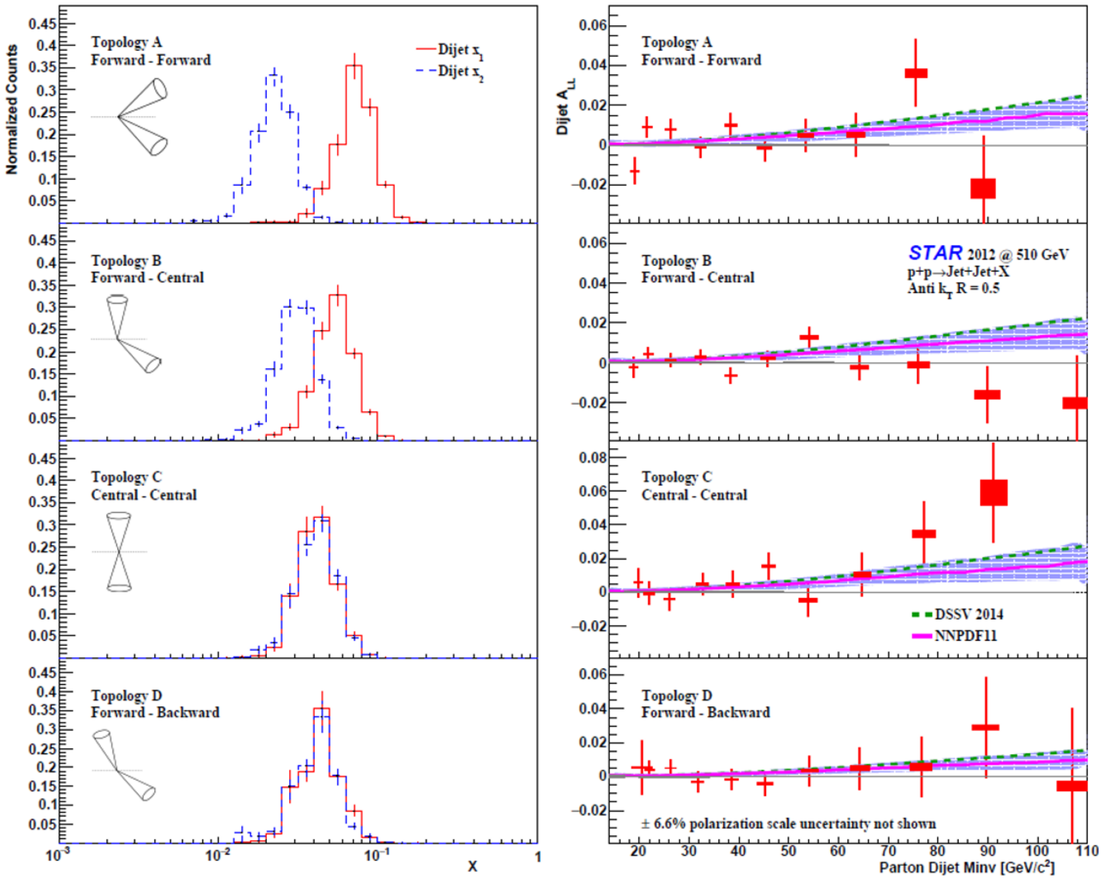

Figure 7: A_{LL} of inclusive dijets as a function of parton dijet invariant mass ($Minv$) at various η topologies. Central corresponds to the pseudorapidity bin $|\eta| < 0.3$ and forward/backward corresponds to $0.3 < |\eta| < 0.9$. Left panel shows the x of the two partons in the various psuedorapidity bins. As you go from forward-forward to central-central and forward-backward the x of the two partons becomes equal. These measurements will help to constrain the shape of $\Delta g(x)$ [6].

5 Transverse Structure of Proton

Transverse momentum dependent PDFs (TMD) are used to go beyond the one-dimensional picture of the nucleon by adding more degrees of freedom. This allows a three-dimensional picture of the proton momentum to be constructed. STAR has made measurements that are sensitive to several of the TMDs, one of which is transversity. The transversity TMD relates the transverse quark spin to the transverse nucleon spin $\delta q(x)$. Transversity is chiral odd and therefore needs an additional chiral-odd function (Collins fragmentation function $H_1^{\perp}$) to be accessible in a physics observable. The Collins asymmetry is the azimuthal distribution of hadrons inside a jet and is defined in equation (5.1)

$$A_{UT}^{sin(\phi_s-\phi_h)} = \frac{d\sigma^{\uparrow} - d\sigma^{\downarrow}}{d\sigma^{\uparrow} + d\sigma^{\downarrow}} \tag{5.1}$$

Here ϕ_s is the angle of the proton spin with respect to the proton-jet momentum plane and ϕ_h is the angle of the jet-pion momentum plane to the proton-jet momentum plane as depicted in Fig. 8; $d\sigma^{\uparrow(\downarrow)}$ is the cross section when spin is up (down) with respect to the proton momentum. The Collins asymmetry for $p^{\uparrow} + p \rightarrow jet + \pi^{\pm} + X$ at $\sqrt{s} = 500$ GeV at $0 < \eta < 1$ is shown in Fig. 9, where z is the fractional hadron momentum to the jet momentum i.e. $z = \frac{\text{hadron momentum}}{\text{jet momentum}}$. The asymmetry is with respect to the azimuthal distribution of pions inside jets. Figure 9 shows the asymmetry growing as z increases which is the first sign that TMDs survive at high Q^2 [7].

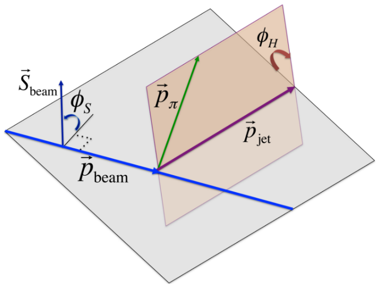

Figure 8: The angles used in the Collins asymmetry definition in equation (5.1) [7].

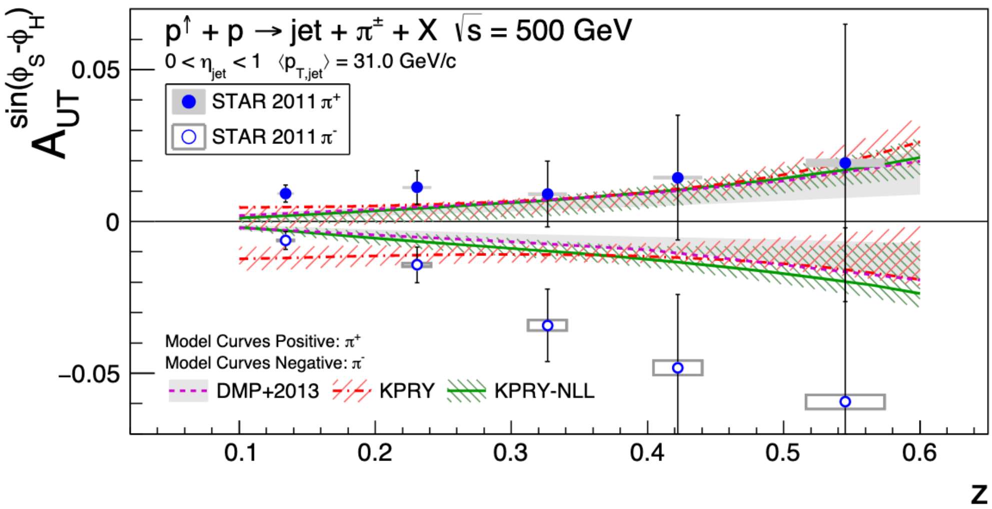

Figure 9: Measured Collins asymmetry A_{UT} as a function of z. This shows the first sign that TMDs survive at high Q^2 [7].

6 STAR Forward Upgrade Capabilities

To improve and expand on the measurements already discussed, STAR is in the process of upgrading several detector subsystems. RHIC data as of 2009 show $\int_{0.05}^{1} \Delta g dx \sim 0.2 \pm^{0.06}_{0.07}$ at $Q^2 = 10$ GeV^2 which is also depicted as the light blue band in Fig. 10. The dark blue band in Fig. 10 shows a projection with RHIC data up to and including the 2015 run. In order to constrain $\Delta g(x)$ at lower x either one has to go to higher $\sqrt{s}$, which is not feasible at RHIC, or larger pseudorapidity. The STAR forward upgrade will do the latter and extend STAR's forward capabilities in the region $2.5 < \eta < 4.0$ to go to lower x. Figure 11 shows the projected x_1 and x_2 for inclusive dijets with the proposed upgrade. In addition, the Collins asymmetry measurement shown in Fig. 9 can also be improved. Figure 12 shows the projected Collins asymmetry precision as well as the asymmetries

Detector	pp and pA	AA
EM calorimeter	$\sim 10\%/\sqrt{E}$	$\sim 20\%/\sqrt{E}$
Hadron calorimeter	$\sim 60\%/\sqrt{E}$	
Tracking system	Charge separation; photon suppression	$0.2 < p_T < 2$ GeV/c with 20-30% $* 1/p_T$

Table 1: Table of hardware requirements for STAR forward upgrade to achieve physics goals

obtained from transversity extractions for one jet p_T and psuedorapidity bin [8]. The black triangle points represent the uncertainties while the red curve indicates the asymmetries for π^+ and the blue curve indicates π^-. In fact, this projection shows only one of several x and Q^2 bins that the STAR forward upgrade will be able to access. Figure 13 shows both the current data on TMDs, which come from DIS experiments, and the projected x and Q^2 accessible with the STAR forward upgrade at RHIC as black filled squares. At $\sqrt{s} = 500$ GeV the new kinematic coverage of STAR will range from 0.05 to 0.5 in x and 10 to 100 GeV^2 in Q^2. In order to accomplish these tasks, the forward upgrade requires a tracking system to deliver good electron-hadron separation, as well as electromagnetic and hadronic calorimeters to provide hadron, π^0, and photon identification. Table 1 shows the individual requirements broken down by species and hardware performance [8].

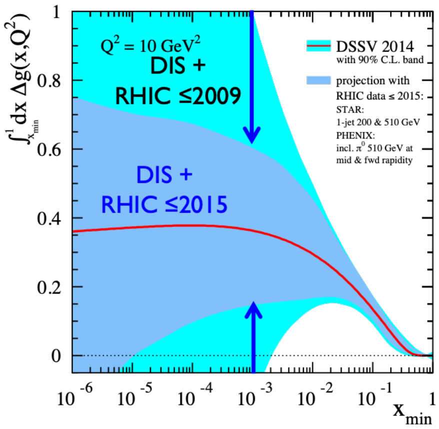

Figure 10: ΔG from DIS and RHIC data in light blue until 2009. Projected ΔG from RHIC data up to and including 2015 in darker blue.

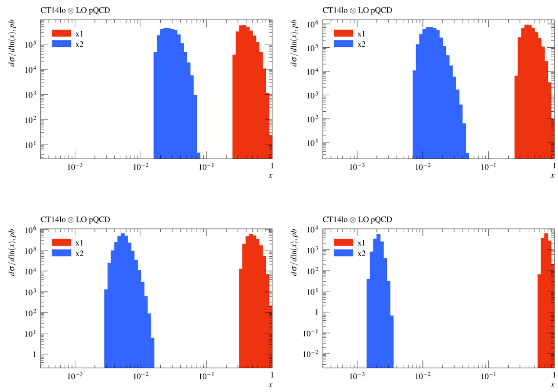

Figure 11: The projected dijet x_1 and x_2 range to be accessed by the STAR forward upgrade, where x_1 and x_2 are defined in equation (4.4).

7 STAR Forward Upgrade Design

The design of the STAR forward upgrade side view can be seen in Fig. 14. It spans $2.5 < \eta < 4.0$ with nearly 2π coverage. The trackers consist of three layers of silicon disks and 4 layers of small-strip Thin Gap Chamber (sTGC). The calorimeters consist of a preshower, an electromagnetic calorimeter (ECal), and a hadronic calorimeter (HCal).

The silicon disks will be located between 140 to 170 cm from the STAR interaction region (IR). Each disk contains 12 modules. They consist of an inner and outer portion that are connected via mechanical structures. A cooling system will also be installed. The sTGC modules consist of 4

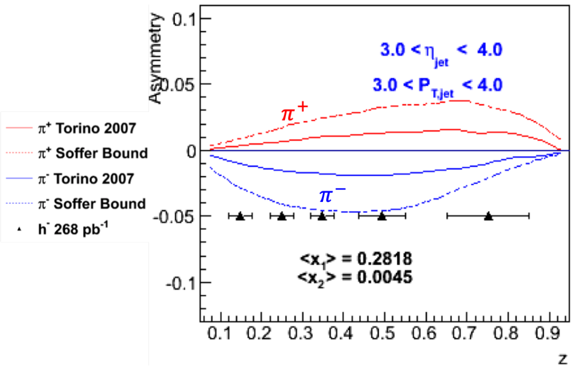

Figure 12: Projected Collins asymmetry uncertainties with pion asymmetries based on transversity extractions as a function of fractional energy z. The projected asymmetry uncertainties are the black triangles with the asymmetries of π^+ in red and π^- in blue. Solid and dashed designate the two different extractions. Only one jet p_T and pseudorapidity bin is shown.

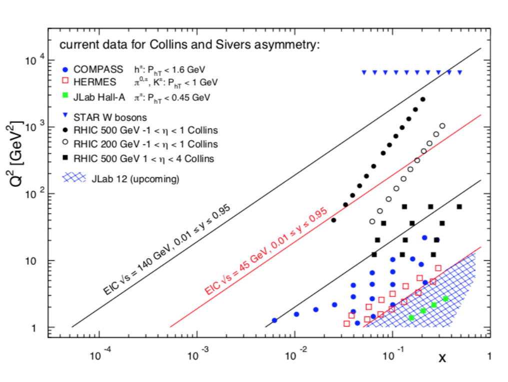

Figure 13: Current TMD data from SIDIS with the STAR forward upgrade projected region of coverage in black squares. One set of the black squares ($x = 0.05$ and $Q^2 = 10\,\mathrm{GeV}^2$) represents the kinematic region for which the Collins asymmetry was projected as shown in Fig. 12.

layers and will be located between 270 to 370 cm. Each layer is double sided to provide x, y and diagonal (45° with respect to x, y) coordinates. It has a position resolution of about 100 μm. It has almost 2π coverage as there needs to be room for the beam pipe support. The sTGC uses the same technology as the ATLAS design [9].

The ECal is a Pb/Sc sandwich that was repurposed from PHENIX. It has been modified to use SiPM readout. It is split into two halves that are located on North side of STAR (right of blue going beam) and South side of STAR (left of blue going beam) with no coverage above and below the beam pipe. It is positioned 7 m from the STAR IR and at a slight angle so that the front face of the ECal is oriented towards the IR to mitigate incident angle effects at this distance. It is $18X_0$ lengths long. The preshower will be a scintillator hodoscope. The hadronic calorimeter will be used for the first time at STAR and needs to be built from scratch. It is a steel (Fe) scintillator (Sc) sandwich with 20 mm Fe/3 mm Sc. It will also utilize SiPM readout and will be located directly behind the EM calorimeter and can be seen in Fig. 14. It is $\sim 4.5\lambda$ long and the lateral size of each HCal tower is 10x10 cm^2, i.e. one HCal tower covers an area roughly equal to a 2x2 set of towers in ECal [8].

8 Conclusions

STAR has made key measurements that have helped in our understanding of the proton structure. Results from longitudinally polarized pp collisions have shown a clear sea quark polarization asymmetry. Also, they have provided constraints for the magnitude of the gluon polarization and the shape of $\Delta g(x)$ using inclusive jets, and dijets at mid-rapidity. Measurements of the Collins asymmetry have shown the first sign that TMDs survive at high Q^2. The STAR forward upgrade plans to both improve on these measurements as well as explore a region of x and Q^2 that has yet to be probed with any facility. The STAR forward upgrade will accomplish this by installing a new tracking system and a new calorimeter system. This upgrade will utilize the newest available technology and build on RHIC and STAR's unique capabilities to carry out measurements in polarized pp collisions.

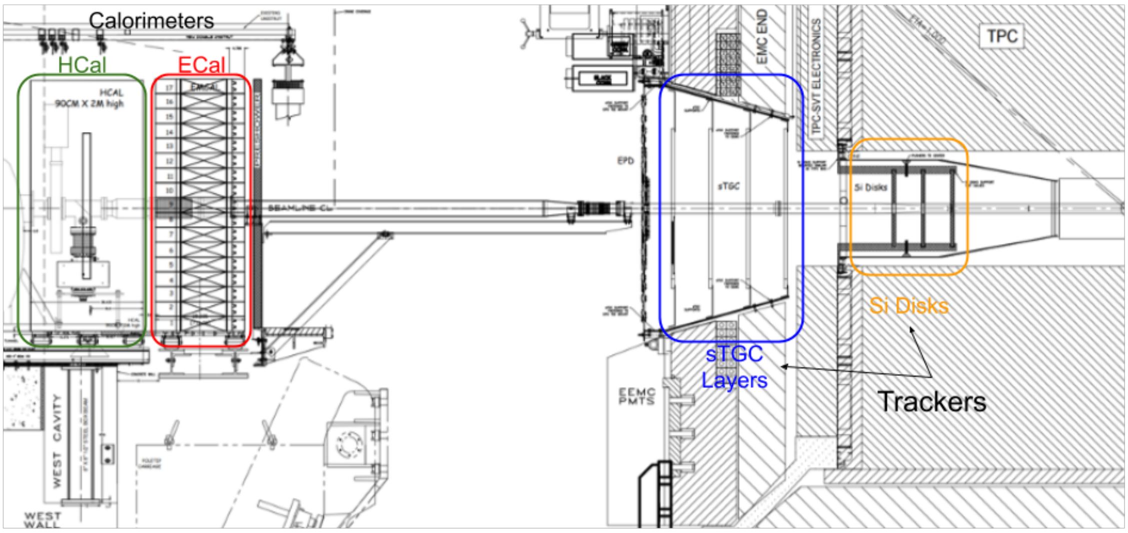

Figure 14: Side view of proposed STAR forward upgrade showing the various components to be installed and some of their details.

References

[1] E.-C. Aschenauer, C. Aidala, A. Bazilevsky, M. Diehl, R. Fatemi, C. Gagliardi, Z. Kang, Y. V. Kovchegov, J. Jalilian-Marian, J. Lajoie, D. V. Perepelitsa, R. Seidl, R. Sassot, E. Sichter-mann, M. Stratmann, S. Trentalange, W. Vogelsang, A. Vossen, and P. Zurita, *The RHIC Cold QCD Plan for 2017 to 2023: A Portal to the EIC*, arXiv:1602.03922.

[2] H. Hahn, E. Forsyth, H. Foelsche, M. Harrison, J. Kewisch, G. Parzen, S. Peggs, E. Raka, A. Ruggiero, A. Stevens, S. Tepikian, P. Thieberger, D. Trbojevic, J. Wei, E. Willen, S. Ozaki, and S. Y. Lee, *The RHIC design overview*, *Nuclear Instruments and Methods in Physics Research Section A: Accelerators, Spectrometers, Detectors and Associated Equipment* **499** (2003), no. 2 245–263.

[3] K. H. Ackermann et al., *STAR detector overview*, *Nuclear Instruments and Methods in Physics Research Section A: Accelerators, Spectrometers, Detectors and Associated Equipment* **499** (2003), no. 2 624–632.

[4] M. Anderson et al., *The STAR time projection chamber: a unique tool for studying high multiplicity events at RHIC*, *Nuclear Instruments and Methods in Physics Research Section A: Accelerators, Spectrometers, Detectors and Associated Equipment* **499** (mar, 2003) 659–678.

[5] **STAR** Collaboration, J. Adam et al., *Measurement of the longitudinal spin asymmetries for weak boson production in proton-proton collisions at* $\sqrt{s} = 510$ *GeV*, *Physical Review D* **99** (mar, 2019) 051102, [arXiv:1812.04817].

[6] **STAR** Collaboration, J. Adam et al., *Longitudinal double-spin asymmetry for inclusive jet and dijet production in pp collisions at* $\sqrt{s} = 510$ *GeV*, *Phys. Rev. D* **100** (sep, 2019) 52005, [arXiv:1906.02740].

[7] **STAR** Collaboration, L. Adamczyk et al., *Azimuthal transverse single-spin asymmetries of inclusive jets and charged pions within jets from polarized-proton collisions at* $\sqrt{s} = 500$ *GeV*, *Phys. Rev. D* **97** (aug, 2017) 32004, [arXiv:1708.07080].

[8] **STAR** Collaboration, *The STAR Forward Calorimeter System and Forward Tracking System beyond BES-II*. https://drupal.star.bnl.gov/STAR/starnotes/public/sn0648.

[9] A. Abusleme et al., *Performance of a full-size small-strip thin gap chamber prototype for the ATLAS new small wheel muon upgrade*, *Nuclear Instruments and Methods in Physics Research, Section A: Accelerators, Spectrometers, Detectors and Associated Equipment* **817** (may, 2016) 85–92, [arXiv:1509.06329].